2023 IEEE 43rd International Conference on Distributed Computing Systems Workshops (ICDCSW) | 979-8-3503-2812-7/23/$31.00 ©2023 IEEE | DOI: 10.1109/ICDCSW60045.2023.00012

Execution and Statistical Arbitrage with Signals in Multiple Automated Market Makers

Álvaro Cartea *Oxford-Man Institute of Quantitative Finance*
Mathematical Institute, University of Oxford
Oxford, United Kingdom
alvaro.cartea@maths.ox.ac.uk Fayçal Drissi *Oxford-Man Institute of Quantitative Finance*
Oxford, United Kingdom
faycal.drissi@eng.ox.ac.uk Marcello Monga *Oxford-Man Institute of Quantitative Finance*
Mathematical Institute, University of Oxford
Oxford, United Kingdom
marcello.monga@maths.ox.ac.uk

***Abstract*—Automated market makers (AMMs) are a new type of trading venue where the rules for liquidity provision and liquidity taking are considerably different from those of the traditional electronic trading venues. AMMs have become one of the key markets to trade crypto-currencies, whose liquidity is highly fragmented and prices exhibit high levels of cointegration. In this paper, we derive the optimal strategy for a liquidity taker (LT) who trades orders of large size and executes statistical arbitrages in a basket of crypto-currencies whose constituents co-move. The LT uses market signals and exchange rate information from relevant AMMs and traditional venues to enhance the performance of her strategy. We use stochastic control tools to derive a closed-form strategy that can be computed and implemented by the LT in real time. Finally, we use market data from two pools of Uniswap v3 and from the LOB-based exchange Binance to study co-movements between crypto-currencies and lead-lag effects between trading venues, and to showcase the performance of the strategy.**

***Index Terms*—Decentralised finance, automated market making, algorithmic trading, statistical arbitrage, predictive signals, market impact, adaptive strategies, smart contracts.**

I. Introduction

Automated market makers (AMMs) are open-source immutable programs that run on peer-to-peer permissionless networks. These programs encode the trading rules that govern how liquidity takers (LTs) and liquidity providers (LPs) interact. The emergence of these trading venues poses great challenges to traditional financial services because they do not rely on traditional intermediaries and stakeholders such as banks and brokers. At present, the most popular type of AMM is the constant product market maker (CPMM) such as Uniswap v3, and AMMs serve mainly as trading venues for crypto-currencies. CPMMs are a special type of constant function market maker (CFMM), where a convex trading function and a set of rules determine how the exchange operates.

The literature on the optimal design of these venues and the mathematical tools to optimally take and provide liquidity are new. In [1], the authors propose models for LTs that trade in a CPMM when prices form in the pool and when the prices form in an alternative venue. In [2], the authors characterise the wealth of LPs in CFMMs and in CPMMs with concentrated liquidity, and provide dynamic LP strategies. The work of [3] uses traditional market making models to propose a new design of AMMs. In [4] and [5] the authors show that LPs can strategically exploit their beliefs on future exchange rates, and study the implications on smart contract design. Finally, the work in [6] and [7] uses convex optimisation for routing and multi-asset trading in CFMMs, and [8] proposes new designs for AMMs.

In practice, LTs usually trade in multiple assets simultaneously. At present, it is key for LTs that trade in CPMMs to consider exchange rates from more liquid alternative venues where prices are formed, and to take into account the significant co-movements that crypto-currencies exhibit. In this work, we solve the problem of an LT who wishes to execute large orders in multiple assets. She has access to different CPMM pools and uses information from exchange rates from alternative trading venues (oracle), and from a set of predictive signals; see [9], [10] for the use of signals in optimal trading.

We formulate the optimal trading problem as a stochastic control problem where the LT controls the speed at which she trades in the different pools. Key to the performance of the trading strategy, is to balance price risk and execution costs. In CPMMs, the execution costs are approximated with the convexity of the trading function, which is a function of the pool's depth and the pool's exchange rate; see [1]. In our model, the joint dynamics of the CPMM rates, the oracle rates, and a set of predictive signals follow a multi-dimensional Ornstein-Uhlenbeck process (multi-OU). Multi-OU dynamics are well-suited to capture (i) the common stochastic trends that crypto-currencies usually share, (ii) the lead-lag effects between oracle and pool rates, and (iii) to incorporate predictive signals.

The remainder of this paper is organised as follows. Section II recalls how LTs and LPs interact with a CPMM, and uses Uniswap v3 data to study the cointegrated dynamics

2332-5666/23/$31.00 ©2023 IEEE
DOI 10.1109/ICDCSW60045.2023.00012

of oracle and pool rates for ETH and BTC. Section III introduces the optimal trading model and derives a closed-form approximation strategy. Section IV implements the model of Section III using oracle rates from Binance and pool rates from Uniswap v3 for an agent in charge of a portfolio composed of the crypto-currencies ETH and BTC.

II. Automated market making

In this section, we first discuss how CFMMs operate and characterise their execution costs and the market impact of liquidity taking activity. Next, we use transaction data to study the co-movements of the exchange rates of ETH and BTC (against USDC) in the CPMM Uniswap v3 and in the more liquid LOB-based venue Binance.

A. Constant function market makers

In a CFMM, LPs and LTs interact through liquidity pooling. LPs deposit assets in a common pool, and LTs trade directly with the pool. In the remainder of this paper, we consider n assets $\boldsymbol{Y} = \left(Y^1, \ldots, Y^n\right)^\intercal$ that are valued in terms of a reference asset X. Moreover, we consider a CFMM that offers a pool for every pair $\left(X, Y^i\right)$, and we refer to the instantaneous exchange rate of Y^i in terms of X in the pool by Z^i.

The liquidity pool for a pair $\left(X, Y^i\right)$ consists of a quantity $x > 0$ of asset X and a quantity $y > 0$ of asset Y^i. The CFMM pool is characterised by a trading function $f(x, y)$, which is differentiable, has convex level sets, and is increasing in both x and y. A CFMM pool imposes an LT trading condition and an LP trading condition both of which define the state of the pool after an LT transaction and after an LP operation is completed.

a) ***LT trading condition****:* Let (x, y) be the state of the pool before the arrival of an LT buy order for a quantity $\Delta y > 0$ of asset Y^i. The quantity $\Delta x > 0$ of asset X that the LT pays to the pool is determined by the LT trading condition $f(x, y) = f(x + \Delta x, y - \Delta y) = \kappa^2$, where $\kappa > 0$ is the *depth* of the pool. For a sell order, the LT trading condition is $f(x, y) = f(x - \Delta x, y + \Delta y) = \kappa^2$. As in [1], [2], we define the *level function* φ as $x = \varphi(y)$, which is differentiable, convex, and decreasing.[1] Moreover, the instantaneous exchange rate is given by

$$Z = -\varphi'(y) \,. \tag{1}$$

The authors in [1] show that one can use a Taylor expansion to approximate the execution costs for trading a quantity Δy with the convexity of φ, so that

$$\left| Z - \tilde{Z}(\Delta y) \right| \approx \frac{1}{2} \varphi''(y) \, |\Delta y| = \frac{1}{\kappa} Z^{3/2} |\Delta y| \,, \tag{2}$$

where $\tilde{Z}(\Delta y)$ is the execution rate. The level function φ is decreasing and convex, thus the execution rate received by an LT deteriorates (i.e., execution costs increase) as the size of the trade increases, and as the depth of the pool κ decreases.

[1]To ensure that the pool cannot be depleted by LT trades, the level function should also satisfy $\lim_{y \to 0} \varphi(y) = +\infty$ and $\lim_{y \to +\infty} \varphi(y) = 0$.

Pair	Volume Uniswap	Volume Binance	Depth Uniswap
ETH/USDC	$\$\, 129.8 \times 10^9$ (1 txn per 13 sec)	$\$\, 267.44 \times 10^9$ (1 txn per 0.13 sec)	2.04×10^7
BTC/USDC	$\$\, 5.088 \times 10^9$ (1 txn per 381 sec)	$\$\, 358.37 \times 10^9$ (1 txn per 1.49 sec)	1.32×10^6

TABLE I: Volume, trading frequency, and depth in Uniswap v3 and Binance for the pairs ETH/USDC and BTC/USDC between 1 January 2022 and 30 June 2022.

Finally, following an LT trade of size Δy, the *price impact* is the difference between the two rates, i.e., $-\varphi'(y \pm \Delta y) + \varphi'(y)$. Using (1) and a Taylor's expansion we write

$$\text{Price impact} \approx \varphi''(y) \, |\Delta y| = \frac{2 \, Z^{3/2}}{\kappa} |\Delta y| \,.$$

b) ***LP trading condition****:* LPs interact with the pool by depositing assets in the pool or withdrawing assets from the pool. The LP trading condition requires that LP operations do not impact the rate Z. However, LP operations do change the depth κ of the pool. More precisely, let (x, y) be the state of the pool before an LP deposits liquidity $(\Delta x, \Delta y)$,[2] so $(x + \Delta x, y + \Delta y)$ is the state of the pool after the deposit, which increases the depth of the pool, because

$$f(x + \Delta x, y + \Delta y) = \overline{\kappa}^2 > f(x, y) = \kappa^2 \,;$$

recall that the trading function is increasing.

Next, let φ_κ be the level function corresponding to the depth κ and let $\varphi_{\overline{\kappa}}$ be the level function corresponding to the depth $\overline{\kappa}$. The LP trading condition requires that when an LP deposits the quantities (x, y) such that $f(x + \Delta x, y + \Delta y) = \overline{\kappa}^2$, then the following equality must hold:

$$Z = -\varphi'_\kappa(y) = -\varphi'_{\overline{\kappa}}(y + \Delta y) \,. \tag{3}$$

B. Cointegration and oracle rates

In this section, we use data from the Uniswap v3 pools USDCETH 0.05% and BTC/USDC 0.3%, and from the LOB-based market Binance for the same pairs, to study the joint dynamics of crypto-currencies in both markets between 1 January 2022 and 30 June 2022. Uniswap v3 is a CPMM with concentrated liquidity running on the Ethereum blockchain, which is a type of distributed ledger technology that validates and stores transactions. At present, it is the most liquid CPMM. In CPMMs, the trading function is $f(x, y) = x \times y$, so the level function is $\varphi(y) = \kappa^2 / y$ and the instantaneous exchange rate is $Z = -\varphi'(y) = \kappa^2 / y^2 = x / y$. Binance is the most liquid LOB-based exchange for all pairs of crypto-currencies, and the venue where prices are formed. Table I shows descriptive statistics, and Figure 1 shows the rates for both BTC and ETH in terms of USDC in the pools we consider. The figure suggests that the exchange rates share common stochastic trends.

Figure 2 shows the dynamics of the pool and oracle rates during a trading day and showcases the lead-lag relationship between both trading venues for a specific day, and suggests

[2]Here, $\Delta x \geq 0$ and $\Delta y \geq 0$.

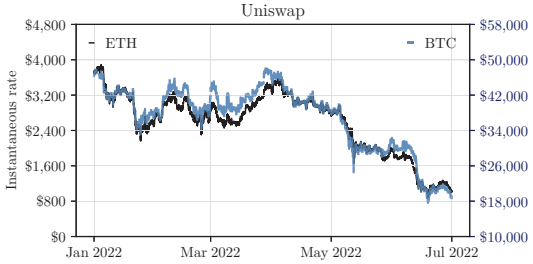

Fig. 1: Exchange rates USDC/ETH and USDC/BTC in Uniswap v3 between January 2022 and June 2022.

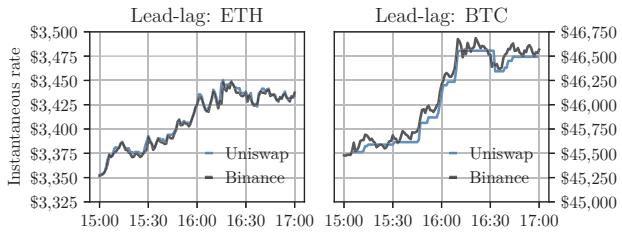

Fig. 2: Exchange rates BTC/USDC and ETH/USDC in Uniswap v3 and Binance between 15:00 and 17:00 on 1 April 2022.

that the information from the oracle rates, i.e., those in Binance in our case, can be used to enhance the trading performance of an LT in the CPMM Uniswap v3. Thus, it is key for an LT who trades multiple crypto-currencies to account for external information from similar assets and from other trading venues.

In our model, we capture the joint dynamics of the pool rates and the oracle rates using a multi-OU process. This process is suited to capture equilibrium relationships as those exhibited between BTC and ETH, and to capture lead-lag effects between different trading venues as those exhibited between Uniswap and Binance. The lead-lad effects are encoded in the cointegration factors in the mean-reversion matrix, which drives the deterministic and long-term component of the process.

To further study the suitability of the multi-OU process, we use the data described above to perform a Johansen's cointegration Trace test for the vector $\boldsymbol{R} = \left(Z^1, Z^2, S^1, S^2\right)$, where Z^1 and S^1 are the pool and oracle rates of ETH, and Z^2 and S^2 are the pool and oracle rates of BTC. The Johansen's test rejects the hypothesis of no cointegration and the hypothesis of a cointegration rank $r = 1$, but does not reject a cointegration rank $r = 2$; see [11] for more details.

The results suggest that the cointegration vectors are $(1, -0.022, -1.002, 0.022)$ and $(1, 0.09, -1.004, -0.088)$. The cointegration vectors, and hence the mean-reversion matrix (i.e., the matrix $\boldsymbol{\beta}$ in (4)), capture the joint dynamics of BTC and ETH, but also the lead-lag relation between the pool rates and oracle rates. Table II shows the results for the Johansen's cointegration Trace test.

Null Hypothesis	Trace statistics	Critical Value	Result
$r \leq 0$	$11,196.97$	54.68	Rejected
$r \leq 1$	$4,821.52$	35.46	Rejected
$r \leq 2$	11.45	19.93	Not rejected

TABLE II: Johansen's cointegration Trace test results (critical values are given for a significance level of 99%). The test confirms a cointegration rank $r = 2$.

III. Optimal portfolio trading with oracles and signals

In this section, an investor is in charge of liquidating a large position in a basket of n risky and cointegrated assets $\boldsymbol{Y} = \left(Y^1, \ldots, Y^n\right)$ in a CPMM. The CPMM offers n pools for each asset against a reference asset X and we denote by $(\boldsymbol{Z}_t)_{t\in[0,T]} = \left(Z^1, \ldots, Z^n\right)_{t\in[0,T]}$ the exchange rates in these pools. The investor uses n oracle rates $(\boldsymbol{S}_t)_{t\in[0,T]} = \left(S^1, \ldots, S^n\right)_{t\in[0,T]}$ from another more liquid exchange and a set of m predictive signals $(\boldsymbol{I}_t)_{t\in[0,T]} = \left(I^1, \ldots, I^m\right)_{t\in[0,T]}$.

The investor must liquidate her initial inventory $\tilde{\boldsymbol{y}}_0 \in \mathbb{R}^n$ over a period of time $[0, T]$ and her wealth is valued in terms of asset X. The joint dynamics of the pool rates $\boldsymbol{Z}$, the oracle rates $\boldsymbol{S}$, and the signals $\boldsymbol{I}$ are modelled by a $2n+m$-dimensional vector $(\boldsymbol{R}_t)_{t\in[0,T]}$ that follows multi-OU dynamics

$$d\boldsymbol{R}_t = \boldsymbol{\beta}\left(\boldsymbol{\mu} - \boldsymbol{R}_t\right) dt + \boldsymbol{\sigma}^\intercal \, d\boldsymbol{W}_t \,, \tag{4}$$

where we force the first n components of $\boldsymbol{R}$ to coincide with $\boldsymbol{Z}$, $\boldsymbol{\beta}$ is a $2n + m \times 2n + m$ mean-reversion matrix, $\boldsymbol{\mu}$ is a $2n + m$-dimensional vector that models the long-term unconditional mean, $\boldsymbol{\sigma}^\intercal$ is the Cholesky decomposition of the asset prices correlation matrix $\boldsymbol{\Sigma}$, the symbol $^\intercal$ denotes the transpose operator, and $(\boldsymbol{W}_t)_{t\in[0,T]}$ is a $2n + m$-dimensional Brownian motion with independent coordinates. For previous work with multi-OU price dynamics see [12], [13], [14].

The investor trades at a continuous n-dimensional speed $(\boldsymbol{\nu}_t)_{t\in[0,T]}$ and the dynamics of her holdings are given by

$$d\tilde{\boldsymbol{y}}_t = -\boldsymbol{\nu}_t \, dt \,. \tag{5}$$

We do not restrict the speed to be positive; if for some $i \in \{1, \ldots, n\}$ we have $\nu^i > 0$ the investor sells asset Y^i and if $\nu^i < 0$ the investor buys the asset.

As discussed above, the rate impact of the LT's activity is encoded in the trading function $f(x, y)$ and is a function of the trading speed as in traditional execution models (see [15]), the pool rate $\boldsymbol{Z}$, and the pool depth κ; see [1].

More precisely, for each asset Y^i, we write the difference between the execution rate $\tilde{Z}^i$ and the instantaneous rate Z^i as

$$\tilde{Z}^i - Z^i = -\frac{\eta}{\kappa^i}\left(Z^i\right)^{3/2} \nu^i \,, \tag{6}$$

where κ^i is the depth of the pool that offers liquidity for the pair $\left(X, Y^i\right)$. Thus, the dynamics of the investor's cash in terms of asset X are given by

$$d\tilde{x}_t = \tilde{\boldsymbol{Z}}_t^\intercal \, \boldsymbol{\nu}_t \, dt = \left(\boldsymbol{Z}_t - \mathfrak{D}\left(\frac{\eta}{\boldsymbol{\kappa}} \odot \boldsymbol{Z}_t^{3/2}\right) \boldsymbol{\nu}_t\right)^\intercal \boldsymbol{\nu}_t \, dt \,, \tag{7}$$

where $\boldsymbol{\kappa}$ is the n-dimensional vector of the depth of the pools, η is a parameter which depends on the investor's trading frequency, $\mathfrak{D}(\boldsymbol{c})$ denotes a diagonal matrix whose diagonal elements are equal to the vector $\boldsymbol{c}$, and $\odot$ denotes the component-wise product. Compared with previous works in the literature that employ multi-OU price dynamics, here market impact is a deterministic function.

Let $\boldsymbol{\mathcal{X}}$ be a $n \times 2n+m$ matrix with $\boldsymbol{\mathcal{X}}_{ij} = \mathbb{1}_{\{i=j\}}$ which maps the first n elements of a $2n+m$-dimensional vector into an n dimensional vector, and write (7) in terms of the vector $\boldsymbol{R}$ as

$$d\tilde{x}_t = \left(\boldsymbol{\mathcal{X}}\,\boldsymbol{R}_t - \mathfrak{D}\left(\frac{\eta}{\boldsymbol{\kappa}} \odot \left(\boldsymbol{\mathcal{X}}\,\boldsymbol{R}_t^{3/2}\right)\right)\boldsymbol{\nu}_t\right)^{\intercal} \boldsymbol{\nu}_t\, dt\,. \tag{8}$$

A. Performance criterion and value function

In our model, the investor maximises her expected terminal wealth in units of X while penalising inventory in the risky assets $\boldsymbol{Y}$. The set of admissible strategies is

$$\mathcal{A}_t = \left\{ (\boldsymbol{\nu}_s)_{s\in[t,T]} \;\middle|\; \begin{array}{l} \mathbb{R}^n\text{-valued, } \mathbb{F}\text{-adapted} \\ \displaystyle\int_t^T \|\boldsymbol{\nu}_s\|^2\, ds < +\infty, \quad \text{a.s.} \end{array} \right\}, \tag{9}$$

and we write $\mathcal{A} := \mathcal{A}_0$. Let $\boldsymbol{\nu} \in \mathcal{A}$, the performance criterion of the investor who trades at speed $\boldsymbol{\nu}$, is

$$u^{\boldsymbol{\nu}}(t,\tilde{x},\tilde{\boldsymbol{y}},\boldsymbol{R}) = \mathbb{E}_{t,\tilde{x},\tilde{\boldsymbol{y}},\boldsymbol{R}}\Big[\tilde{x}_T^{\boldsymbol{\nu}} + \boldsymbol{R}_T^{\intercal}\,\boldsymbol{\mathcal{X}}^{\intercal}\,\tilde{\boldsymbol{y}}_T^{\boldsymbol{\nu}} - (\tilde{\boldsymbol{y}}_T^{\boldsymbol{\nu}})^{\intercal}\,\boldsymbol{\alpha}\,\tilde{\boldsymbol{y}}_T^{\boldsymbol{\nu}} - \phi\int_t^T (\tilde{\boldsymbol{y}}_s^{\boldsymbol{\nu}})^{\intercal}\,\tilde{\boldsymbol{\Sigma}}\,\tilde{\boldsymbol{y}}_s^{\boldsymbol{\nu}}\, ds\Big], \tag{10}$$

and the investor's value function is

$$u(t,\tilde{x},\tilde{\boldsymbol{y}},\boldsymbol{R}) = \sup_{\nu\in\mathcal{A}} u^{\nu}(t,\tilde{x},\tilde{\boldsymbol{y}},\boldsymbol{R})\,. \tag{11}$$

The first term on the right-hand side of (10) is the terminal cash of the LT in terms of asset X. The second term represents the terminal value of her remaining inventory marked-to-market using the pool rates $\boldsymbol{Z}$. The third term is a 'cost' from liquidating the terminal inventory $\tilde{\boldsymbol{y}}_T$ at time T. The magnitude of this cost is encoded in the diagonal positive matrix $\boldsymbol{\alpha}$. Finally, the last term is a running inventory penalty where $\tilde{\boldsymbol{\Sigma}}$ is the covariance matrix of the pool rates $\boldsymbol{Z}$, and the parameter $\phi \geq 0$ quantifies the urgency of the investor to liquidate inventory.[3]

The value function solves the Hamilton–Jacobi–Bellman (HJB) equation

$$\begin{aligned} 0 =& \partial_t w - \phi\,\tilde{\boldsymbol{y}}^{\intercal}\tilde{\boldsymbol{\Sigma}}\,\tilde{\boldsymbol{y}} + (\boldsymbol{\mu}-\boldsymbol{R})^{\intercal}\boldsymbol{\beta}\,\partial_{\boldsymbol{R}} w \\ &+ \frac{1}{2}\,\mathrm{Tr}\left(\boldsymbol{\Sigma}\,D_{\boldsymbol{RR}} w\right) + \sup_{\nu\in\mathbb{R}^n}\Bigg(-\boldsymbol{\nu}^{\intercal}\partial_{\tilde{\boldsymbol{y}}} w \\ &+ \left(\boldsymbol{\mathcal{X}}\,\boldsymbol{R} - \mathfrak{D}\left(\frac{\eta}{\boldsymbol{\kappa}} \odot \left(\boldsymbol{\mathcal{X}}\,\boldsymbol{R}^{3/2}\right)\right)\boldsymbol{\nu}\right)^{\intercal}\boldsymbol{\nu}\,\partial_{\tilde{x}} w\Bigg), \end{aligned} \tag{12}$$

with terminal condition

$$w(T,\tilde{x},\tilde{\boldsymbol{y}},\boldsymbol{R}) = \tilde{x} + \boldsymbol{R}^{\intercal}\,\boldsymbol{\mathcal{X}}^{\intercal}\,\tilde{\boldsymbol{y}} - \tilde{\boldsymbol{y}}^{\intercal}\,\boldsymbol{\alpha}\,\tilde{\boldsymbol{y}}\,. \tag{13}$$

[3]The units of ϕ are such that the penalty is in units of X.

Next, substitute the ansatz

$$w(t,\tilde{x},\tilde{\boldsymbol{y}},\boldsymbol{R}) = \tilde{x} + \boldsymbol{R}^{\intercal}\,\boldsymbol{\mathcal{X}}^{\intercal}\,\tilde{\boldsymbol{y}} + \theta(t,\tilde{\boldsymbol{y}},\boldsymbol{R})\,, \tag{14}$$

into (12) and solve the first order condition to obtain the partial differential equation (PDE)

$$\begin{aligned} 0 =\; & \partial_t\theta - \phi\,\tilde{\boldsymbol{y}}^{\intercal}\tilde{\boldsymbol{\Sigma}}\,\tilde{\boldsymbol{y}} + (\boldsymbol{\mu}-\boldsymbol{R})^{\intercal}\boldsymbol{\beta}\,(\boldsymbol{\mathcal{X}}^{\intercal}\tilde{\boldsymbol{y}} + \partial_{\boldsymbol{R}}\theta) \\ &+ \frac{1}{2}\,\mathrm{Tr}\left(\boldsymbol{\Sigma}\,D_{\boldsymbol{RR}}\theta\right) + \partial_{\tilde{\boldsymbol{y}}}\theta^{\intercal}\,\mathfrak{D}\left(\frac{\boldsymbol{\kappa}}{4\,\eta} \odot \left(\boldsymbol{\mathcal{X}}\,\boldsymbol{R}^{-3/2}\right)\right)\partial_{\tilde{\boldsymbol{y}}}\theta\,, \end{aligned} \tag{15}$$

with terminal condition

$$\theta(T,\tilde{x},\tilde{\boldsymbol{y}},\boldsymbol{R}) = -\tilde{\boldsymbol{y}}^{\intercal}\,\boldsymbol{\alpha}\,\tilde{\boldsymbol{y}}\,, \tag{16}$$

where the optimal trading speed in feedback form is

$$\nu^{\star} = -\mathfrak{D}\left(\frac{\boldsymbol{\kappa}}{2\,\eta} \odot \left(\boldsymbol{\mathcal{X}}\,\boldsymbol{R}^{-3/2}\right)\right)\partial_{\tilde{\boldsymbol{y}}}\theta\,. \tag{17}$$

The semi-linear PDE (15) does not admit a closed-form solution. In practice, one uses a numerical scheme to approximate the solution θ and deduce the optimal speed (17). In our model, the dimensionality of the problem grows exponentially with the number of assets. As a consequence, numerical schemes suffer from the curse of dimensionality.

In practice, the performance of an execution or statistical arbitrage strategy heavily relies on the ability to compute and send liquidity taking instructions with minimal latency. Thus, it is crucial for an investor to employ a trading strategy that is relatively fast to compute. Hence, we derive a closed-form approximation strategy for (17) which can be implemented and tracked by the investor in real time. Therefore, we extend a method developed in [1] for a single asset framework.

Subsection III-B solves an execution problem when convexity costs are fixed for a value of the pool rate Z, and Subsection III-C defines the closed-form approximation strategy as the uniform limit of a family of these strategies.

B. Optimal strategy with deterministic execution costs

Here, we derive a trading strategy that assumes a deterministic and fixed cost parameter in (6). More precisely, consider here that the execution cost in (6) is

$$\tilde{\boldsymbol{Z}} - \boldsymbol{Z} = -\eta\,\mathfrak{D}(\boldsymbol{\zeta})\,\boldsymbol{\nu}\,. \tag{18}$$

Here the n-dimensional vector $\boldsymbol{\zeta} > 0$ is a fixed cost parameter. Our aim is to derive the optimal strategy $\left(\boldsymbol{\nu}_t^{\star,\boldsymbol{\zeta}}\right)_{t\in[0,T]}$ for a given value of the parameter $\boldsymbol{\zeta} > 0$. For each value of $\boldsymbol{\zeta}$, we consider the set of admissible strategies $\mathcal{A}_t^{\boldsymbol{\zeta}}$ similar to that in (9) and we write $\mathcal{A}^{\boldsymbol{\zeta}} := \mathcal{A}_0^{\boldsymbol{\zeta}}$. Let $\boldsymbol{\nu}^{\boldsymbol{\zeta}} \in \mathcal{A}^{\boldsymbol{\zeta}}$. For an LT who trades at speed $\left(\boldsymbol{\nu}_t^{\boldsymbol{\zeta}}\right)_{t\in[0,T]}$, the inventory $\left(\tilde{\boldsymbol{y}}_t^{\boldsymbol{\zeta}}\right)_{t\in[0,T]}$ evolves as

$$d\tilde{\boldsymbol{y}}_t^{\boldsymbol{\zeta}} = -\boldsymbol{\nu}_t^{\boldsymbol{\zeta}}\,dt\,, \tag{19}$$

and the LT's cash follow the dynamics

$$d\tilde{x}_t^{\boldsymbol{\zeta}} = \left(\boldsymbol{\mathcal{X}}\,\boldsymbol{R}_t - \eta\,\mathfrak{D}\left(\boldsymbol{\zeta}\right)\,\boldsymbol{\nu}_t^{\boldsymbol{\zeta}}\right)^{\intercal}\boldsymbol{\nu}_t^{\boldsymbol{\zeta}}\,dt\,. \tag{20}$$

We consider the same performance criterion as that in (10) and let $u_{\boldsymbol{\zeta}}$ be the value function of the investor. To solve the new optimisation problem for each value of $\boldsymbol{\zeta}$, follow the

same steps as above to obtain the PDE verified by $\theta_{\boldsymbol{\zeta}}$, where $w_{\boldsymbol{\zeta}}(t,\tilde{x},\tilde{\boldsymbol{y}},\boldsymbol{R}) = \tilde{x} + \boldsymbol{R}^\intercal\,\boldsymbol{\mathcal{X}}^\intercal\,\tilde{\boldsymbol{y}} + \theta_{\boldsymbol{\zeta}}(t,\tilde{\boldsymbol{y}},\boldsymbol{R})$, and write

$$\begin{aligned} 0 =& \partial_t\theta_{\boldsymbol{\zeta}} - \phi\,\tilde{\boldsymbol{y}}^\intercal\,\tilde{\boldsymbol{\Sigma}}\,\tilde{\boldsymbol{y}} + (\boldsymbol{\mu}-\boldsymbol{R})^\intercal\,\boldsymbol{\beta}\,(\boldsymbol{\mathcal{X}}^\intercal\,\tilde{\boldsymbol{y}} + \partial_{\boldsymbol{R}}\theta_{\boldsymbol{\zeta}}) \\ &+ \frac{1}{2}\,\mathrm{Tr}\left(\boldsymbol{\Sigma}\,D_{\boldsymbol{RR}}\theta_{\boldsymbol{\zeta}}\right) + \frac{1}{4\,\eta}\,\partial_{\tilde{\boldsymbol{y}}}\,\theta_{\boldsymbol{\zeta}}^\intercal\,\mathfrak{D}\left(\boldsymbol{\zeta}\right)^{-1}\,\partial_{\tilde{\boldsymbol{y}}}\theta_{\boldsymbol{\zeta}}\,, \end{aligned} \tag{21}$$

with terminal condition

$$\theta_{\boldsymbol{\zeta}}(T,\tilde{x},\tilde{\boldsymbol{y}},\boldsymbol{R}) = -\tilde{\boldsymbol{y}}^\intercal\boldsymbol{\alpha}\,\tilde{\boldsymbol{y}}\,, \tag{22}$$

where the investor's optimal trading speed in feedback form is

$$\nu^{\boldsymbol{\zeta},\star} = -\frac{1}{2\,\eta}\,\mathfrak{D}\left(\boldsymbol{\zeta}\right)^{-1}\,\partial_{\tilde{\boldsymbol{y}}}\theta_{\boldsymbol{\zeta}}\,. \tag{23}$$

To further study the problem, substitute the ansatz

$$\begin{aligned} \theta_{\boldsymbol{\zeta}}(t,\tilde{x},\tilde{\boldsymbol{y}},\boldsymbol{R}) =& \tilde{\boldsymbol{y}}^\intercal A_{\boldsymbol{\zeta}}(t)\,\tilde{\boldsymbol{y}} + \tilde{\boldsymbol{y}}^\intercal B_{\boldsymbol{\zeta}}(t)\,\boldsymbol{R} + C_{\boldsymbol{\zeta}}(t)\,\tilde{\boldsymbol{y}} \\ &+ \boldsymbol{R}^\intercal D_{\boldsymbol{\zeta}}(t)\,\boldsymbol{R} + E_{\boldsymbol{\zeta}}(t)\,\boldsymbol{R} + F_{\boldsymbol{\zeta}}(t)\,, \end{aligned} \tag{24}$$

in (21) to obtain the system of ODEs

$$\begin{cases} 0 = & A'_{\boldsymbol{\zeta}}(t) - \phi\,\tilde{\boldsymbol{\Sigma}} + \frac{1}{\eta}A_{\boldsymbol{\zeta}}(t)^\intercal\mathfrak{D}\left(\boldsymbol{\zeta}\right)^{-1}A_{\boldsymbol{\zeta}}(t)\,, \\ 0 = & B'_{\boldsymbol{\zeta}}(t) - \boldsymbol{\mathcal{X}}\,\boldsymbol{\beta}^\intercal - B_{\boldsymbol{\zeta}}(t)\,\boldsymbol{\beta}^\intercal \\ & \quad + \frac{1}{\eta}\,A_{\boldsymbol{\zeta}}(t)^\intercal\,\mathfrak{D}\left(\boldsymbol{\zeta}\right)^{-1}B_{\boldsymbol{\zeta}}(t)\,, \\ 0 = & C'_{\boldsymbol{\zeta}}(t) + \boldsymbol{\mu}^\intercal\,\boldsymbol{\beta}\,\boldsymbol{\mathcal{X}}^\intercal + \boldsymbol{\mu}^\intercal\,\boldsymbol{\beta}B_{\boldsymbol{\zeta}}(t)^\intercal \\ & \quad + \frac{1}{\eta}\,C_{\boldsymbol{\zeta}}(t)^\intercal\,\mathfrak{D}\left(\boldsymbol{\zeta}\right)^{-1}A_{\boldsymbol{\zeta}}(t)\,, \\ 0 = & D'_{\boldsymbol{\zeta}}(t) + \frac{1}{4\,\eta}B_{\boldsymbol{\zeta}}(t)^\intercal\,\mathfrak{D}\left(\boldsymbol{\zeta}\right)^{-1}B_{\boldsymbol{\zeta}}(t)\,, \\ 0 = & E'_{\boldsymbol{\zeta}}(t) - E_{\boldsymbol{\zeta}}(t)^\intercal\,\boldsymbol{\beta}^\intercal + \frac{1}{2\,\eta}\,C_{\boldsymbol{\zeta}}(t)^\intercal\,\mathfrak{D}\left(\boldsymbol{\zeta}\right)^{-1}\,B_{\boldsymbol{\zeta}}(t)\,, \\ 0 = & F'_{\boldsymbol{\zeta}}(t) + \boldsymbol{\mu}^\intercal\,\boldsymbol{\beta}E_{\boldsymbol{\zeta}}(t) + Tr\left(\boldsymbol{\Sigma}\,D_{\boldsymbol{\zeta}}(t)\right) \\ & \quad + \frac{1}{4\,\eta}\,C_{\boldsymbol{\zeta}}(t)^\intercal\,\mathfrak{D}\left(\boldsymbol{\zeta}\right)^{-1}C_{\boldsymbol{\zeta}}(t)\,, \end{cases} \tag{25}$$

with terminal condition

$$\begin{aligned} A_{\boldsymbol{\zeta}}(T) &= -\boldsymbol{\alpha}\,, \\ B_{\boldsymbol{\zeta}}(T) = C_{\boldsymbol{\zeta}}(T) =& D_{\boldsymbol{\zeta}}(T) = E_{\boldsymbol{\zeta}}(T) = F_{\boldsymbol{\zeta}}(T) = 0\,. \end{aligned} \tag{26}$$

The ODEs in D, E, F, and the corresponding terminal conditions admit the unique solutions $D_{\boldsymbol{\zeta}} = E_{\boldsymbol{\zeta}} = F_{\boldsymbol{\zeta}} = 0$. Next, use the classical tools for Riccati equations to show that the ODE for $A_{\boldsymbol{\zeta}}(t)$ admits the unique solution

$$A_{\boldsymbol{\zeta}}(t) = \eta\,\mathfrak{D}\left(\boldsymbol{\zeta}\right)^{\frac{1}{2}}\left(\boldsymbol{\Psi} + \boldsymbol{\xi}\left(t\right)^{-1}\right)\,\mathfrak{D}\left(\boldsymbol{\zeta}\right)^{\frac{1}{2}}\,, \tag{27}$$

where

$$\begin{cases} \boldsymbol{\Psi} & = \frac{\phi}{\eta}\,\mathfrak{D}\left(\boldsymbol{\zeta}\right)^{-\frac{1}{2}}\,\tilde{\boldsymbol{\Sigma}}\,\mathfrak{D}\left(\boldsymbol{\zeta}\right)^{-\frac{1}{2}}\,, \\ \boldsymbol{\xi}\left(t\right) & = -\frac{\boldsymbol{\Psi}^{-1}}{2}\left(I - e^{-2\boldsymbol{\Psi}(T-t)}\right) \\ & \quad -e^{-\boldsymbol{\Psi}(T-t)}\left(\boldsymbol{\Phi}+\boldsymbol{\Psi}\right)^{-1}e^{-\boldsymbol{\Psi}(T-t)}, \\ \boldsymbol{\Phi} & = \frac{1}{\eta}\mathfrak{D}\left(\boldsymbol{\zeta}\right)^{-\frac{1}{2}}\,A_{\boldsymbol{\zeta}}(T)\,\mathfrak{D}\left(\boldsymbol{\zeta}\right)^{-\frac{1}{2}}\,. \end{cases} \tag{28}$$

Finally, use Theorem 3 in [12] to obtain the unique solution for $B_{\boldsymbol{\zeta}}$ and $C_{\boldsymbol{\zeta}}$. More precisely, observe that $C_{\boldsymbol{\zeta}} = -\boldsymbol{\mu}^\intercal\,B_{\boldsymbol{\zeta}}^\intercal$ and write

$$B_{\boldsymbol{\zeta}}(t) = \int_t^T \boldsymbol{:}\,e^{\int_t^u(\boldsymbol{\beta}^\intercal - \frac{1}{\eta}A_{\boldsymbol{\zeta}}(s)^\intercal\mathfrak{D}(\boldsymbol{\zeta})^{-1})\,ds}\boldsymbol{:}\,\boldsymbol{\mathcal{X}}\boldsymbol{\beta}^\intercal\,du\,, \tag{29}$$

where the notation $\boldsymbol{:}\,e^{\int_t^u\cdot\,ds}\boldsymbol{:}$ denotes the time-ordered exponential.

Thus, we obtain a closed-form solution to the HJB equation and an analytical formula for the optimal trading speed in the case of fixed execution costs. In particular, substitute (24) into (23) to obtain the optimal strategy in feedback form

$$\nu^{\boldsymbol{\zeta},\star} = \frac{1}{2\,\eta}\,\mathfrak{D}\left(\boldsymbol{\zeta}\right)^{-1}\,\left(B_{\boldsymbol{\zeta}}(t)^\intercal\,(\boldsymbol{\mu}-\boldsymbol{R}) - 2\,\boldsymbol{A}_{\boldsymbol{\zeta}}(t)\,\tilde{\boldsymbol{y}}\right). \tag{30}$$

C. Closed-form approximation strategy

When the execution cost parameter $\boldsymbol{\zeta}$ in the optimal strategy (30) is set to $\boldsymbol{Z}^{3/2}/\boldsymbol{\kappa}$, with the observed pool rates $\boldsymbol{Z}\in\mathbb{R}^n$, then the strategy derived in the previous section approximates the optimal strategy (23).

Here, we use a first order approximation of the optimal speed to define the closed-form approximation strategy. More precisely, we use the strategy (30) with $\boldsymbol{\zeta} = \boldsymbol{Z}^{3/2}/\boldsymbol{\kappa}$ to approximate the optimal strategy (17). We write, with a slight abuse of notation, $\boldsymbol{A}(t,\boldsymbol{\zeta})$ and $\boldsymbol{B}(t,\boldsymbol{\zeta})$, and propose the closed-form approximation strategy

$$\begin{aligned} \nu^\star = \frac{1}{2\,\eta}\,\mathfrak{D}\left(\boldsymbol{\zeta}\right)^{-1}\,&\left(B\left(t,\boldsymbol{\kappa}^{-1}\odot\boldsymbol{Z}^{3/2}\right)^\intercal\,(\boldsymbol{\mu}-\boldsymbol{R})\right. \\ &\left. - 2\,\boldsymbol{A}\left(t,\boldsymbol{\kappa}^{-1}\odot\boldsymbol{Z}^{3/2}\right)\,\tilde{\boldsymbol{y}}\right). \end{aligned} \tag{31}$$

The first term on the right-hand side of (31) is a speculative component of the strategy – it adjusts the speed of trading to the difference between the long-term unconditional mean $\boldsymbol{\mu}$ and the observed rates and signals $\boldsymbol{R}$, where the adjustments are scaled by the mean-reversion matrix $\boldsymbol{\beta}$. The second term is a classical Almgren–Chriss (AC) strategy that adjusts the current inventory as a function of convexity costs $\boldsymbol{\zeta}$ and the urgency parameter ϕ. One can prove that a family of optimal strategies of the form (30) converges uniformly to the closed-form approximation strategy in (31).

IV. Performance analysis

We use transaction data to show the performance of the closed-form approximation strategy in (31). Similar to Section II, we use transaction data for ETH and BTC in two pools of the CPMM Uniswap v3 and the more liquid exchange Binance.

To estimate the execution costs incurred by the LT in the pools we consider, one needs to track the depth of the pool at every instant. We use historical LP operations to reconstruct the historical depth κ of the two pools, which we use to estimate the execution costs during the execution programmes of the LT.

Here, we perform consecutive in-sample estimation of model parameters using 24 hours of transaction data sampled at the minute frequency, and out-of-sample execution of the closed-form approximation strategy (31) using T =12 hours, $\phi = 1\times10^{-6}$, and $\boldsymbol{\alpha} = \begin{pmatrix} 10 & 0 \\ 0 & 10 \end{pmatrix}$.

For each individual run, we compute the optimal strategy and compute the terminal profit and loss of the execution programme, which is $\tilde{\boldsymbol{x}}_T + \tilde{\boldsymbol{y}}_T^\intercal\,\boldsymbol{Z}_T - \tilde{\boldsymbol{y}}_0^\intercal\,\boldsymbol{Z}_0$. Next, we shift both the in-sample and the out-of-sample time windows by 12 hours and repeat the process, thus performing 357 runs in total. In each run, the agent must (randomly with probability $1/2$) either liquidate 1000 units of ETH, and 100 units of BTC, or buy the same amounts.

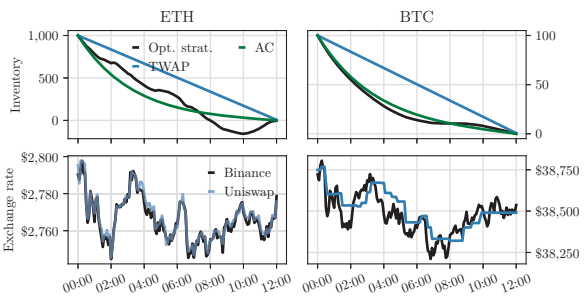

Fig. 3: Inventory in ETH and BTC during the execution programme (top) and the pool and oracle exchange rates (bottom). Model parameters are obtained using data between 00:00 on 1 February and 00:00 on 2 February 2022, and the execution programme is between 00:00 on 2 February and 12:00 on 2 February 2022.

To estimate the coefficients of the process driving the joint dynamics of the exchange rates, we use the VAR(1) model

$$\Delta R_t = a + \Pi\, \Delta R_{t-1} + \epsilon_t\,,$$

which is a time discretisation of our multi-OU process; where $a \in \mathbb{R}^{2n+m}$, $\Pi \in \mathcal{M}_{2n+m}(\mathbb{R})$, and ϵ is white noise. We use in-sample data and a least squares regression to estimate the coefficients of the VAR model, from which one obtains the mean-reversion matrix $\boldsymbol{\beta}$, the long-term unconditional mean $\boldsymbol{\mu}$, and the covariance matrix $\boldsymbol{\Sigma}$.

As an example, Figure 3 shows the optimal inventory when the in-sample data is that of 1 February 2022 and the execution programme is over the following 12 hours. Figure 3 shows that the strategy uses the spread between the oracle rates and the pool rates for both pairs to predict a potential decrease or increase in the rate. The depth of the ETH/USDC 0.05% pool is larger than that of the BTC/USDC 0.3%; see Table I, so trading costs caused by the convexity of the level function are low in the first pool and high in the second. Hence, the speculative component of the closed-form approximation strategy (31) is less exploited in the less liquid pool even though the spread between the oracle and the pool rate is wide.

In our analysis, we compare the performance of our strategy with that of a classical Almgren-Chriss (AC) strategy and a TWAP strategy; see [16]. Moreover, we run the strategy (31) with zero initial inventory, which corresponds to an arbitrage strategy that uses the cointegration factors to take speculative positions. Table III shows the distribution of the terminal P&L for the three strategies and shows that the closed-form approximation strategy outperforms TWAP and AC on average, and is profitable for statistical arbitrage.

V. Conclusions

In this paper, we derived the optimal strategy for a liquidity taker (LT) who trades in an AMM a basket of cryptocurrencies whose constituents co-move. The LT uses market signals and exchange rate information from relevant AMMs and traditional venues to enhance the performance of her strategy. We used stochastic control tools to derive a closed-form strategy that can be computed and implemented by the LT in real time. Finally, we used market data from Uniswap v3 and Binance to study co-movements between cryptocurrencies and lead-lag effects between trading venues, and to showcase the performance of the strategy.

	Avg. P&L	Std. Dev.
Optimal	$ 2,328	$ 54,805
Optimal (stat. arb.)	$ 2,658	$ 5,819
AC	$ -343	$ 54,823
TWAP	$ -3,705	$ 99,946

TABLE III: Average and standard deviation of the terminal P&L with strategy (31) (liquidation and statistical arbitrage) and from executing TWAP and AC for 357 runs of in-sample estimation of model parameters and out-of-sample execution.

References

[1] Á. Cartea, F. Drissi, and M. Monga, "Decentralised finance and automated market making: Execution and speculation," *Available at SSRN 4144743*, 2022.

[2] ——, "Decentralised finance and automated market making: Predictable loss and optimal liquidity provision," *Available at SSRN 4273989*, 2022.

[3] P. Bergault, L. Bertucci, D. Bouba, and O. Guéant, "Automated market makers: Mean-variance analysis of lps payoffs and design of pricing functions," *arXiv preprint arXiv:2212.00336*, 2022.

[4] M. Neuder, R. Rao, D. J. Moroz, and D. C. Parkes, "Strategic liquidity provision in Uniswap v3," 2021.

[5] Z. Fan, F. Marmolejo-Cossío, B. Altschuler, H. Sun, X. Wang, and D. C. Parkes, "Differential liquidity provision in Uniswap v3 and implications for contract design," 2022.

[6] G. Angeris, A. Evans, T. Chitra, and S. Boyd, "Optimal routing for constant function market makers," in *Proceedings of the 23rd ACM Conference on Economics and Computation*, 2022, pp. 115–128.

[7] G. Angeris, A. Agrawal, A. Evans, T. Chitra, and S. Boyd, "Constant function market makers: Multi-asset trades via convex optimization," in *Handbook on Blockchain*. Springer, 2022, pp. 415–444.

[8] Á. Cartea, F. Drissi, L. Sánchez-Betancourt, D. Siska, and L. Szpruch, "Automated market makers designs beyond constant functions," 2023.

[9] M. Forde, L. Sánchez-Betancourt, and B. Smith, "Optimal trade execution for Gaussian signals with power-law resilience," *Quantitative Finance*, vol. 22, no. 3, pp. 585–596, 2022.

[10] Á. Cartea, R. Donnelly, and S. Jaimungal, "Enhancing trading strategies with order book signals," *Applied Mathematical Finance*, vol. 25, no. 1, pp. 1–35, 2018.

[11] S. Johansen, "Estimation and hypothesis testing of cointegration vectors in Gaussian vector autoregressive models," *Econometrica: journal of the Econometric Society*, pp. 1551–1580, 1991.

[12] Á. Cartea, L. Gan, and S. Jaimungal, "Trading co-integrated assets with price impact," *Mathematical Finance*, vol. 29, 08 2018.

[13] P. Bergault, F. Drissi, and O. Guéant, "Multi-asset optimal execution and statistical arbitrage strategies under Ornstein–Uhlenbeck dynamics," *SIAM Journal on Financial Mathematics*, vol. 13, no. 1, 2022.

[14] F. Drissi, "Solvability of differential Riccati equations and applications to algorithmic trading with signals," *Available at SSRN 4308008*, 2022.

[15] Á. Cartea, S. Jaimungal, and J. Penalva, *Algorithmic and High-Frequency Trading*. Cambridge University Press, 2015.

[16] O. Guéant, *The Financial Mathematics of Market Liquidity: From Optimal Execution to Market Making*, 03 2016.